Papers

Abdominal radiographic and ultrasonographic findings in ferrets (*Mustela putorius furo*) with systemic coronavirus infection

E. Dominguez, R. Novellas, A. Moya, Y. Espada, J. Martorell

Ferret systemic coronavirus infection (FSCV) is a systemic disease in ferrets that clinically and pathologically resembles the dry form of FIP. The present study describes abdominal imaging features of 11 ferrets with FSCV. Abdominal survey radiographs were available for eight ferrets and ultrasound examination for all cases. Loss of lumbar musculature, decreased peritoneal detail, presence of mid-abdominal soft-tissue masses and splenomegaly were the most significant radiographic signs in these patients. Ultrasonographic findings including peritonitis, abdominal lymphadenopathy, splenomegaly, abdominal soft-tissue masses, nephromegaly and changes in the renal cortex echogenicity were recorded in the majority of cases with FSCV. As an imaging modality, ultrasound is superior to radiology when abdominal contrast is reduced, as it frequently occurs in these cases. However, although imaging techniques provide additional information in the antemortem diagnosis, they can not replace the definitive diagnosis based on histological and immunohistochemical results.

THREE diseases caused by group 1 coronaviruses have been described in ferrets: severe acute respiratory syndrome (SARS), caused by SARS coronavirus, has been experimentally transmitted to ferrets, although no natural infection has been reported in this species; epizootic catarrhal enteritis (ECE), whose causative agent is the ferret enteric coronavirus (FRECV), is a highly contagious diarrhoeal disease with a mortality of below 5 per cent and ferret systemic coronavirus infection (FSCV), caused by the ferret systemic coronavirus (FRSCV), a new disease characterised by feline infectious peritonitis (FIP)-like clinical signs and lesions (Williams and others 2000, Martínez and others 2006, Murray and others 2010).

It is still not clear whether the ferret systemic coronavirus (FRSCV) is derived from its enteric counterpart (FRECV) by in vivo mutation, is a cocirculating distinct strain or whether the FRSCV has originated as a result of a recombination between FRECV and another group 1 coronavirus (Wise and others 2006, 2010).

Clinical signs observed in FSCV are non-specific. Diarrhoea, weight loss, lethargy, hyporexia or anorexia and vomiting are common features described in these patients. Gastrointestinal signs may lead to loss of body condition and moderate to severe emaciation. Neurological signs, respiratory signs, dehydration and jaundice have also been described. On physical examination, large palpable abdominal masses, splenomegaly and nephromegaly are common findings.

Veterinary Record (2011) 169, 231 doi: 10.1136/vr.d4705

E. Dominguez, DVM, PhD,
R. Novellas, DVM, PhD, DipI ECVDI,
A. Moya, DVM,
Y. Espada, DVM, PhD,
J. Martorell, DVM, PhD, DipI ECZM,
Hospital Clínic Veterinari, Departament de Medicina i Cirurgia Animals, Facultat de Veterinària, Universitat Autònoma de Barcelona, 08193, Spain

Correspondence to Martorell,
e-mail: jaumemiquel.martorell@uab.es

Provenance: not commissioned; externally peer reviewed

Published Online First: 22 August 2011

Typical haematologic signs include non-regenerative anaemia, hyperglobulinaemia (polyclonal hypergammaglobulinaemia), hypoalbuminemia and thrombocytopenia (Murray and others 2010).

Currently, as it occurs in cats, histopathological examination of affected tissues is the gold standard to diagnose FSCV. Widespread granulomas on serosal surfaces and within the parenchyma of abdominal and thoracic organs are observed and coronavirus antigen can be detected by means of immunohistochemistry (IHC) in the cytoplasm of macrophages included in the granulomas (Perpiñán and López 2008, Lewis and O'Brien 2010, Murray and others 2010).

The purpose of the present study was to describe abdominal radiographic and ultrasonograhic features of ferrets with confirmed diagnosis of systemic coronavirus infection.

Materials and methods

The medical records of 11 ferrets diagnosed with FSCV at the 'Hospital Clínic Veterinari-Universitat Autònoma de Barcelona' (HCV-UAB) between 2008 and 2010 were reviewed. The age ranged between five and 24 months, with a median age of 12 months. Four ferrets were female (two neutered and two entire) and seven were male (three neutered and four entire). The weight of the ferrets ranged between 220 to 980 g (median weight 571 g).

Histopathological examination in all the ferrets was performed using routine histology stains (haematoxylin and eosin) and special stains (Ziehl-Neelsen, periodic acid-Schiff [PAS] and Warthin Starry methods) to exclude other infectious aetiologies. The presence of the FRSCV was confirmed by immunohistochemistry. FCV3-70 monoclonal antibody (Custom Monoclonal Internationals) was used to detect feline group 1 coronavirus in the affected tissues, by peroxidase-antiperoxidase method as it has been previously described (Martínez and others 2008).

In all the cases, at least one imaging modality study (radiography or ultrasonography) was performed. The patients were unsedated during the examinations. Diagnostic imaging procedures were performed and reviewed consensually by at least one of the diagnostic imaging service clinicians (ED, YE and RN) and the exotic animal medicine and surgery service clinician (JM).

TABLE 1: Radiographic, ultrasonographic and histopathological findings observed in 11 ferrets (*Mustela putorius furo*) with systemic coronavirus infection

Case		Laboratory findings	Radiographic findings	Ultrasonographic findings	Histopathological findings
1	Neutered ♂ 18 months	Anaemia Neutrophilic leucocytosis Thrombocytopenia Hyperproteinaemia Polyclonal gammopathy	Pendulous ventral abdominal wall Loss lumbar musculature Local decreased serosal detail Local GI tract dilation with gas Splenomegaly Mid-abdominal soft-tissue masses Nephromegaly	Peritonitis Severe splenomegaly Abdominal lymphadenopathy Severe nephromegaly Hydronephrosis Hydroureter Perinephric infiltration Vascular thrombosis	*Granulomatous peritonitis IHC+
2	Neutered ♂ seven months	Neutrophilic leucocytosis Hyperproteinemia Monoclonal gammopathy	Not done	Soft-tissue mass Renal cysts	*Granulomatous lymphadenitis IHC+
3	♂ 12 months	Anaemia Neutrophilic leucocytosis Hyperproteinemia Monoclonal gammopathy	Loss lumbar musculature Diffuse decreased serosal detail Generalised GI tract dilation with gas Moderate splenomegaly	Increased intestinal peristalsis Abdominal lymphadenopathy Renal cysts	Granulomatous lesions in CNS IHC+ Fibronecrotising splenitis
4	Neutered ♂ eight months	Anaemia Neutrophilic leucocytosis Hyperproteinemia Polyclonal gammopathy	Loss lumbar musculature Diffuse decreased serosal detail Local GI tract dilation with gas Mid-abdominal soft-tissue masses	Peritonitis Splenomegaly, Granular parenchyma Mid-abdominal soft-tissue masses Nephromegaly Hyperechoic renal cortex	Granulomatous peritonitis, lymphadenitis, enteritis IHC+ Ectopic spleen Normal kidneys
5	♀ six months	Hyperproteinemia Monoclonal gammopathy	Loss lumbar musculature Local decreased serosal detail Mild splenomegaly Mid-abdominal soft-tissue masses	Peritonitis Abdominal lymphadenopathy Mid-abdominal soft-tissue masses Renal cysts	Granulomatous peritonitis, pancreatitis IHC+ Renal, splenic and pulmonary congestion
6	♂ eight months	Anaemia Polyclonal gammopathy	Pendulous ventral abdominal wall Loss lumbar musculature Local decreased serosal detail Moderate splenomegaly Mid-abdominal soft-tissue masses	Peritonitis Splenomegaly Abdominal lymphadenopathy Mid-abdominal soft-tissue masses	Granulomatous peritonitis, lymphadenitis, nephritis Granulomatous lesions in CNS IHC+ Normal spleen Lymphoplasmacytic coroiditis
7	♀ 18 months	Anaemia Hyperproteinemia Monoclonal gammopathy	Not done	Peritonitis Splenomegaly Abdominal lymphadenopathy Mid-abdominal soft-tissue masses Hyperechoic renal parenchyma Mild pyelectasia	Granulomatous peritonitis, lymphadenitis, nephritis, enteritis Granulomatous infiltration abdominal wall IHC+ Necrosis spleen Lymphoplasmacytic coroiditis
8	♂ five months	Anaemia Thrombocytopenia Hyperproteinemia Monoclonal gammopathy	Loss lumbar musculature Local decreased serosal detail Nephromegaly	Peritonitis Splenomegaly Abdominal lymphadenopathy Nephromegaly Renal cysts	Granulomatous peritonitis, lymphadenitis, pancreatitis, enteritis, nephritis Pyogranulomatous hepatitis, splenitis, pneumonia IHC+ Lymphoid hyperplasia spleen/ extramedullary haematopoiesis
9	♂ 12 months	Anaemia Serum protein electrophoresis not done	Pendulous ventral abdominal wall Loss lumbar musculature Mid-abdominal soft-tissue masses	Peritonitis Abdominal lymphadenopathy Hyperechoic renal cortex Moderate pyelectasia	Granulomatous peritonitis, lymphadenitis, nephritis IHC+
10	Neutered ♀ 24 months	Anaemia Neutrophilic leucocytosis Thrombocytopenia Hyperproteinemia Serum protein electrophoresis not done	Not done	Peritonitis Nephromegaly Hyperechoic renal cortex Hydroureter Moderate pyelectasia Perinephric infiltration	*Granulomatous nephritis IHC+
11	Neutered ♀ 18 months	Anaemia Hyperproteinemia Polyclonal gammopathy	Loss lumbar musculature Diffuse decreased serosal detail	Peritonitis Thickened renal cortex	Granulomatous nephritis Granulomatous lesions in CNS Pyogranulomatous hepatitis IHC+

* Histopathological samples obtained from surgical biopsies. In the other cases, samples were obtained during postmortem examination
GI Gastrointestinal, IHC+ Positive immunohistochemical labelling against group 1 coronavirus

Right lateral and ventrodorsal radiographic views were reviewed for evaluation of the following structures: abdominal wall and extra-abdominal soft-tissue structures, peritoneum and retroperitoneum, gastrointestinal tract (stomach, small bowel and colon), liver, spleen and urogenital system.

Abdominal ultrasonography was performed using a 9 to 13 MHz linear or microconvex phase array transducer. The following features were evaluated: ultrasonographic appearance of the abdominal cavity (peritoneum, omentum and mesentery), presence of abdominal effusion and echogenicity of the effusion, presence of gastrointestinal abnormalities (stomach, small bowel, colon and pancreas), liver and spleen size and echogenicity, presence of abdominal lymphadenopathy and abdominal masses, kidney echogenicity, shape and size.

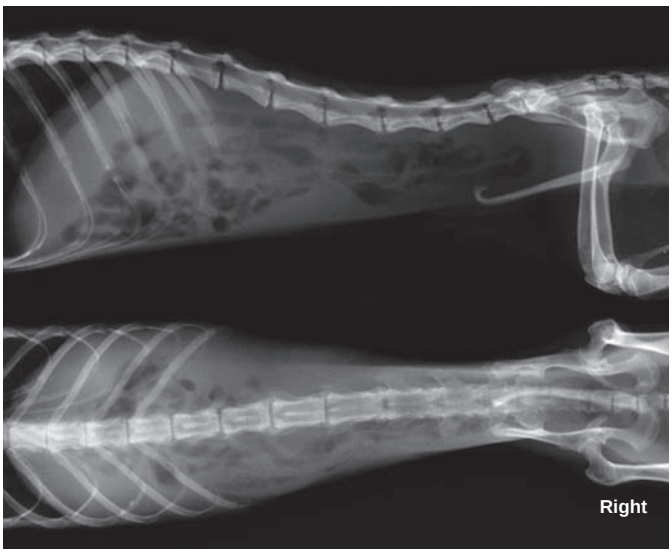

FIG 1: Right lateral and ventrodorsal radiographs of a 12-month-old ferret with a history of lethargy, anorexia and diarrhoea. Note the severe loss of lumbar musculature indicating the poor body condition of the patient

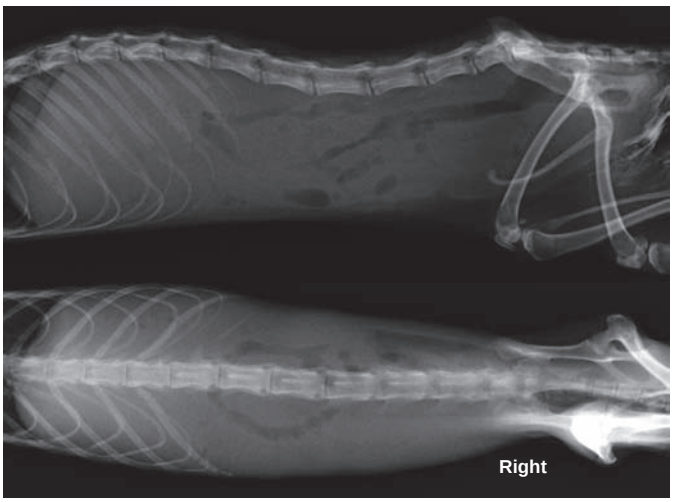

FIG 2: Right lateral and ventrodorsal radiographs of a ferret with hyporexia and lethargy. Note the diffuse, severe, loss of intra-abdominal contrast due to granulomatous peritonitis

Given the limited information available for normal radiographic and ultrasonographic appearance and dimensions of most of the abdominal organs in ferrets, criteria to define normality and abnormality were based on anatomical data previously published (Evans and An 1998, Paul-Murphy and others 1999) and on the authors' experience, including comparison with previously imaged normal ferrets.

Results

Ten ferrets were presented with a clinical history of lethargy, eight with hyporexia or anorexia, six had experienced weight loss, five had diarrhoea and one vomiting. Moderate to severe cachexia was recorded in eight ferrets, abdominal masses were palpated in six animals, abdominal pain and pale mucous membranes were noted in three patients and abdominal distension was observed in two of them. Results of laboratory findings (CBC, serum biochemical analysis and serum biochemical electrophoresis) are described in Table 1.

Radiographic findings

Abdominal survey radiographs were available for eight ferrets (Table 1). In all patients, there was moderate to severe loss of lumbar musculature (Fig 1). Mild to severe pendulous ventral abdominal wall was observed in three of them.

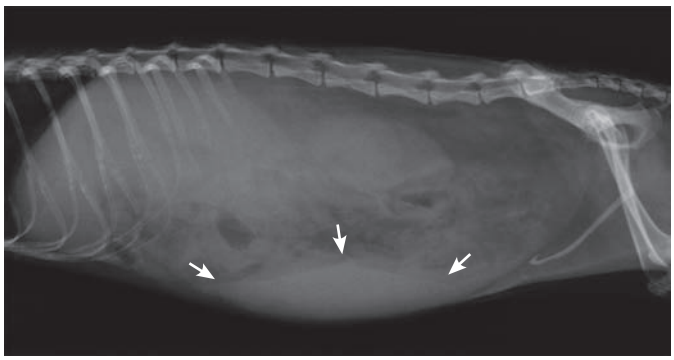

FIG 3: Right lateral radiograph of an 18-month-old ferret with abdominal distension. The spleen was elongated, thick and easily visualised (white arrows)

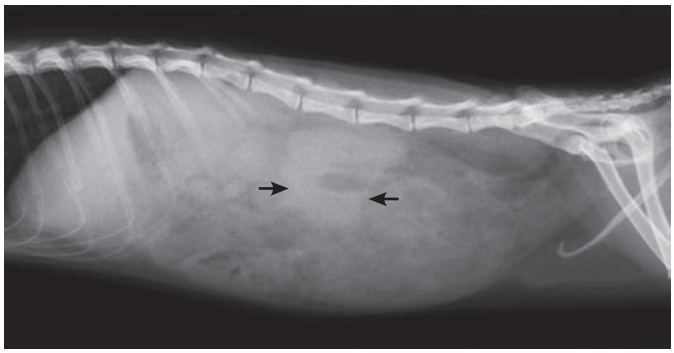

FIG 4: Right lateral radiograph of a ferret with abdominal pain. A soft-tissue mass was identified in the mid-abdomen of this patient (between arrows). granulomatous peritonitis was diagnosed on histology

In seven ferrets, decreased serosal detail was observed in the peritoneum and retroperitoneum (Fig 2). It was located in the cranial and mid-abdomen in four ferrets, whereas a diffuse, moderate to severe loss of intra-abdominal contrast was detected in three cases.

Mild to severe dilation of the gastrointestinal tract with gas was observed in three ferrets. It was generalised in one case (affecting the stomach, small bowel and colon) and located in the small bowel in the other two cases.

The liver was considered radiographically unremarkable in all cases.

Spleen size was abnormal in four ferrets. Diffuse splenomegaly was classified as mild to moderate in three cases and as severe the other one (Fig 3). It was considered that a normal spleen should be located in the left hypogastric region parallel to the greater curvature of the stomach and have relatively sharp well-defined margins. Severe splenomegaly was diagnosed when the caudal border of the spleen was extending beyond the left kidney, when it had rounded margins and it was easy to identify the head and the tail of the spleen in both, lateral and ventrodorsal radiographs and when there was a dorsal displacement of the small intestine in lateral views. Mild to moderate splenomegaly was diagnosed in intermediate conditions.

Mid-abdominal soft-tissue masses were noted in five cases. The exact origin of these masses was difficult to assess because of loss of intra-abdominal serosal detail (Fig 4).

The urogenital system was abnormal in two cases, where severe left nephromegaly without other urinary changes was observed.

Ultrasonographic findings

Abdominal ultrasound was available for all cases (Table 1). Signs consistent with peritonitis, such as the presence of mild to moderate amount of anechoic peritoneal effusion, thickening of the peritoneum, omentum and mesentery and a hyperechoic and hyperattenuating appearance of the abdominal cavity were observed in nine ferrets (Fig 5).

The wall thickness, layering and the luminal content of the gastrointestinal tract were normal in all patients. A single ferret showed increased intestinal peristalsis (continuous contraction of

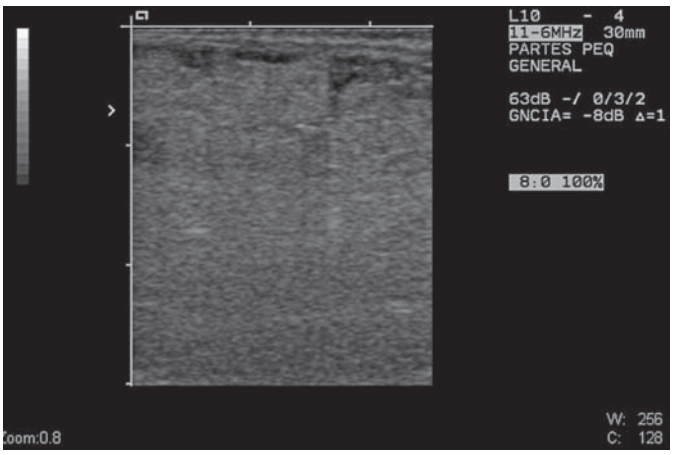

FIG 5: Longitudinal ultrasound image of a ferret with granulomatous peritonitis. Diffuse hyperechoic, irregular and thickened appearance of the peritoneum, omentum and mesentery was recorded in this patient

the small bowel during the ultrasound examination) without other abnormalities.

Liver echogenicity and liver size were normal in all patients. Splenomegaly was found in five ferrets, whereas the echogenicity of the spleen was normal in four of them. One ferret presented a granular, instead of a homogeneous parenchyma.

Abdominal lymphadenopathy was detected in seven ferrets. Mean dimensions (sd) of the mesenteric lymph nodes were 13.17 mm (1.74) in length by 8.32 mm (3.46) in width. Abnormal mesenteric lymph nodes were round to amorphous in shape and showed variable echogenicity. Whereas, normal echogenicity was observed in two animals (Fig 6a) in three cases, the mesenteric lymph nodes showed multiple, diffuse hypoechoic nodules. In another case, they were heterogeneous with a mixed echogenic pattern (Fig 6b), and one presented a central hypoechoic area surrounded by hyperechoic borders.

Ill-defined soft-tissue masses with mixed echogenicity, surrounded by hyperechoic fat, were detected in the abdomen of five ferrets. Mean dimensions (sd) of the abdominal masses were 30.2 mm (7.18) in length by 20.34 mm (2.70) in width. Most of these masses were irregular in shape and showed heterogeneous echotexture (Fig 7). Three of them were highly vascularised.

Renal echogenicity was normal in six cases. One ferret showed a hyperechoic left kidney, which was isoechoic to the spleen and had reduced corticomedullary definition. Three patients presented bilaterally hyperechoic renal cortex (Fig 8) and one ferret showed mildly heterogeneous parenchyma in the caudal pole of the left kidney with a thickened cortex (Fig 9a).

Seven ferrets had normal kidney size (left kidney 25.83 [2.36] x 12.66 [1.28] mm, right kidney 24.22 [1.41] x 12.28 [2.83] mm, values expressed as mean (sd), three of them had moderate bilateral nephromegaly (left kidney 35.68 [4.02] x 16.72 [3.62] mm, right kidney 34.43 [4.15] x 14.89 [4.16] mm) and another showed severe bilateral nephromegaly (left kidney 42.4 x 16.7 mm, right kidney 37.2 x 1.83 mm) with perinephric infiltration (retroperitoneal fat mildly hyperechoic and hyperattenuating). In this case (neutered male), bilateral hydronephrosis (right renal pelvis 6.9 mm, left renal pelvis 4.4 mm) and bilateral hydroureter (luminal diameter of the distended ureters 2.5 mm) were detected. In this patient, the perinephric infiltration extended towards the urinary bladder including the bladder neck and caused thickening of the mesentery, which presented diffuse anechoic to hypoechoic lines. This infiltration was particularly severe at the level of the bladder serosa, which appeared hypoechoic related to the surrounding fat and was markedly thickened and irregular (Fig 10). In this case, neither intraluminal lesions nor mucosal irregularities were detected and the urine remained completely anechoic.

Moderate pyelectasia was observed in two patients (renal pelvis 3 to 3.5 mm). One of them, a neutered female, showed unilateral hydroureter (ureteral distension 4.4 mm) and signs consistent with perinephric infiltration. Mild pyelectasia (renal pelvis 1.10 mm) was

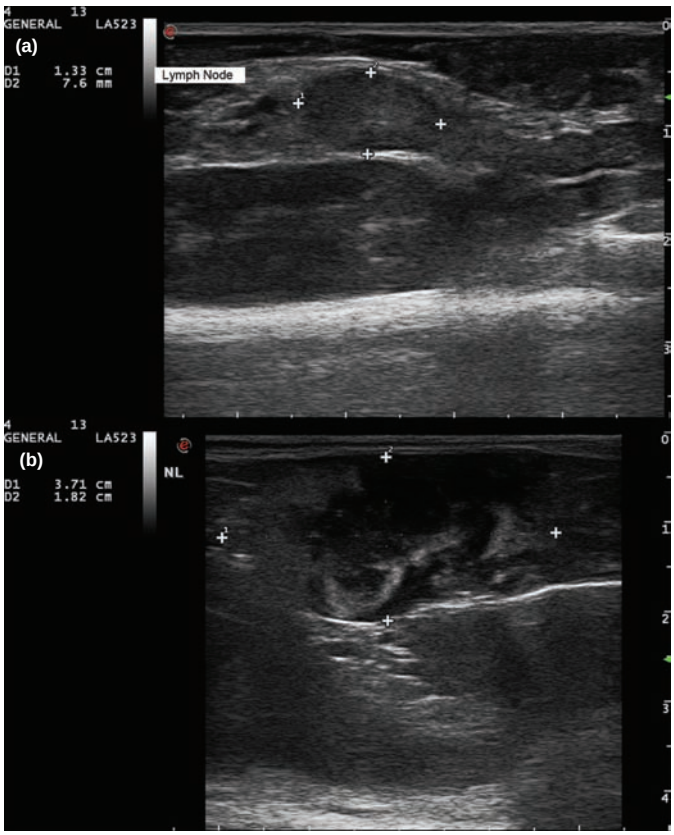

FIG 6: (a) Longitudinal sonographic image of a lymph node (between callipers). This lymph node showed normal echogenicity and echotexture. (b) Markedly enlarged and heterogeneous mesenteric lymph nodes, with hypoechoic and anechoic areas were observed in this patient with pyogranulomatous lymphadenitis (between callipers)

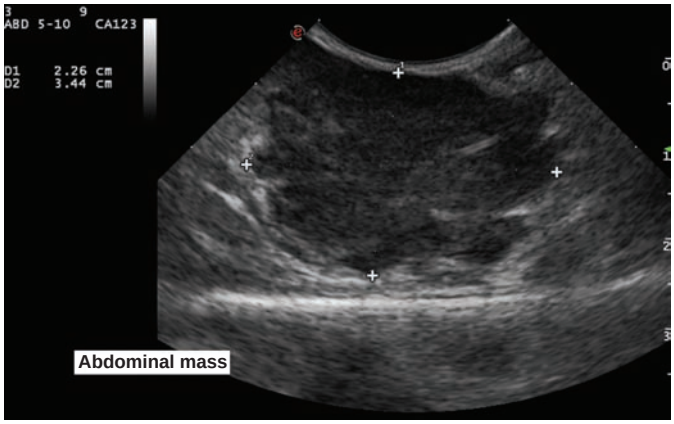

FIG 7: Longitudinal sonographic image of a ferret with vomiting. A large and heterogeneous mass (between callipers) surrounded by hyperechoic fat was scanned in the mid-abdomen of this patient

scanned in a non-neutered female. Other renal findings included the presence of cortical renal cysts (less than 0.5 cm in diameter) in four ferrets, which did not produce renal distortion.

Severe inguinal inflammation characterised by poorly defined hyperechoic subcutaneous tissue with small amounts of anechoic fluid infiltrating between the fascial planes was detected in one ferret. Vascular thrombosis and collateral vessels neoformation were seen in the femoral vein close to the inguinal canal in the same patient (Fig 11).

Histological examination of the affected tissues was available for all cases (surgical biopsy samples from three ferrets and samples of the postmortem examination from the rest). Lesions observed included, granulomatous or pyogranulomatous lymphadenitis, peritonitis, nephritis (Fig 9b), enteritis, pancreatitis, splenitis, hepatitis, pneumonia and granulomatous lesions at the CNS (Table 1) (Figs 12a, 13b).

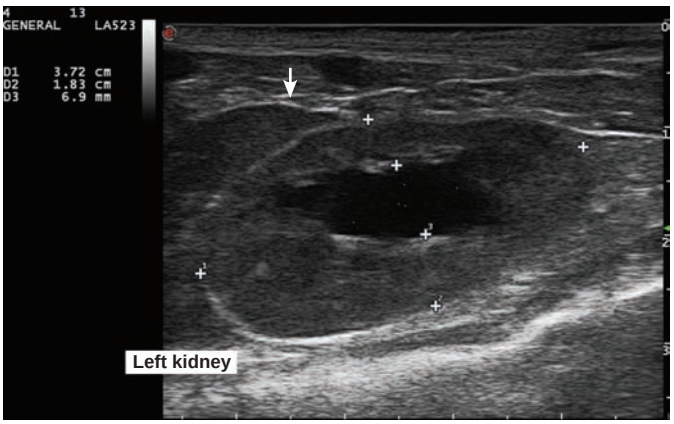

FIG 8: Longitudinal sonographic image of the left kidney of a ferret. The kidney (external callipers) was enlarged and the renal cortex appeared isoechoic to the adjacent spleen (white arrow). The corticomedullary definition was attenuated and the renal pelvis (internal callipers) was dilated (6.9 mm)

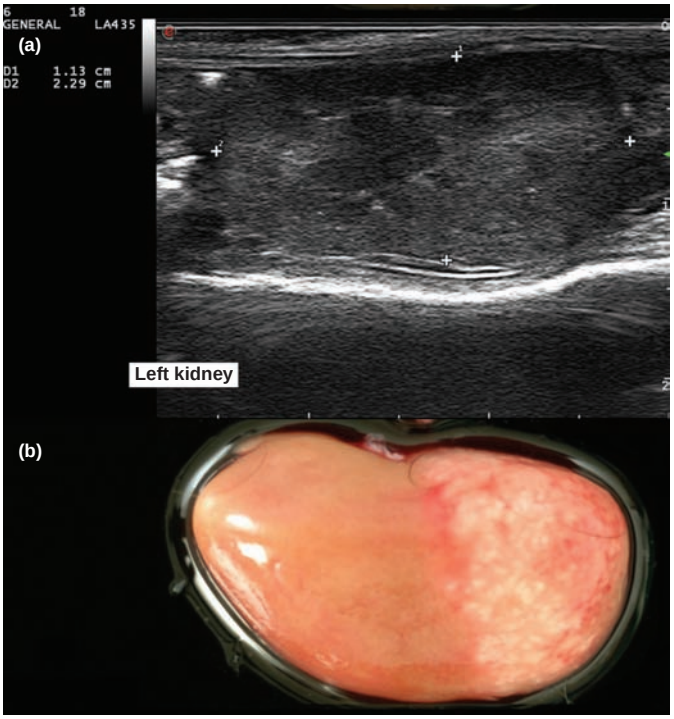

FIG 9: (a) Longitudinal sonographic image of the left kidney of a ferret. The caudal pole showed mildly heterogeneous parenchyma with a thickened cortex. (b) Image from postmortem examination: left kidney of the same ferret showing a whitish, thickened and granular lesion located in the caudal pole of the left kidney

Negative results for special stains – Ziehl-Neelsen, PAS and Warthin Starry stains excluded the presence of other aetiological agents, such as mycobacteria, other bacteria (including *Helicobacter* species.) and fungal organisms.

The presence of coronavirus antigen in the affected tissues was confirmed by means of positive immunohistochemistry against group 1 coronavirus (Table 1) (Figs 12b, 13b).

Discussion

FSCV is an immune-mediated disease, which clinically and pathologically resembles the non-effusive form of FIP. Although laboratory tests, such as RT-PCR assays to detect ferret coronavirus infection and serum antibody tests, have been recently tested in ferrets, there is no a definitive method to diagnose FSCV antemortem (Garner and others 2008, Wise and others 2010). Inclusion criteria for the present study were histopathological and immunohistochemical results consistent with FSCV because they remain the gold standard in the diagnosis of the disease.

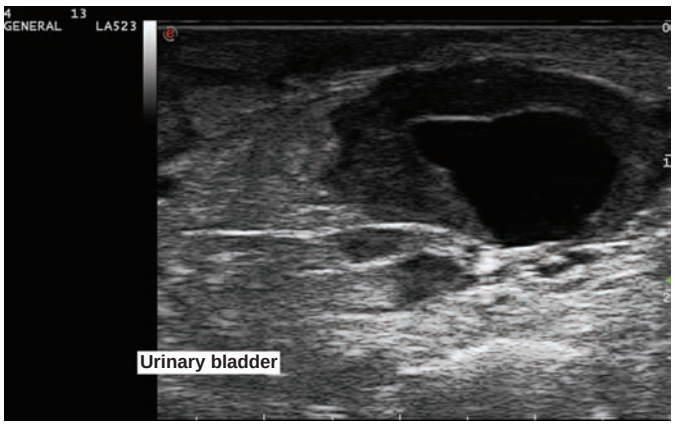

FIG 10: Longitudinal sonographic image of the urinary bladder of a ferret showing a severe inflammatory infiltration of the visceral peritoneum. The inflammatory infiltration extended from the perinephric area towards the bladder neck and the inguinal region

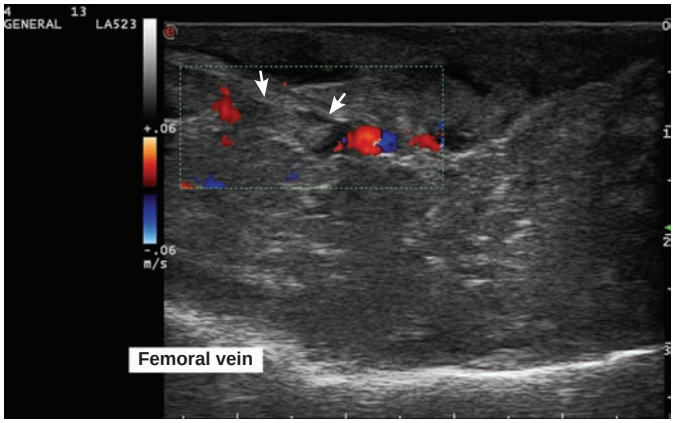

FIG 11: Longitudinal ultrasound image of the femoral vein of a ferret. A well-defined, oval, mildly echogenic thrombus was located in the lumen of the vessel (arrows). No evidence of flow through this point was detected on colour Doppler examination

Age, gender distribution, clinical signs, physical examination and laboratory results of the present population were consistent with previously published data in ferrets (Garner and others 2008, Perpiñán and López 2008, Murray and others 2010). Although, 44 per cent of serum protein electrophoresis showed polyclonal gammopathy, monoclonal gammopathy was encountered in 56 per cent of them. These results differ from other publications in ferrets, where only polyclonal gammopathy has been described. However, it is a common finding in cats with FIP, which may reveal both polyclonal and monoclonal hypergammaglobulinaemia (Garner and others 2008, Perpiñán and López 2008, Addie and others 2009, Murray and others 2010).

Only a reduced amount of information about imaging features in FSCV has been published. Radiographic findings related to FSCV abdominal masses, splenomegaly, nephromegaly and signs consistent with abdominal effusion have been mentioned in general reports (Perpiñán and López 2008, Murray and others 2010). However, ultrasonographic findings of FSCV were not available in the literature. As it was expected, ultrasonographic signs observed in the current study were similar to those found in cats with FIP (Lewis and O'Brien 2010).

The loss of intra-abdominal contrast seen radiographically in the present study may be explained by different causes. When this was generalised, it may have been caused by the lack of peritoneal and retroperitoneal fat secondary to emaciation or by the presence of peritoneal effusion and/or peritonitis. When focal, it may have been caused by a mass effect secondary to abdominal lymphadenopathy or by the presence of granulomatous lesions (Thrall 2007, Farrow 2009, Dennis 2010). These features were confirmed by means of ultrasonography.

Cats affected with the effusive form of FIP usually have anechoic abdominal effusion, consistent with pure or modified transudates. Echogenic effusion may also be occasionally seen in cats (Lewis and O'Brien 2010). In this report, only a minimal amount of anechoic effusion was detected on the ultrasound scan of eight ferrets, which correlates well with the fact that FSCV infrequently produces effusions into the body cavities, in contrast to the effusive form of FIP (Murray and others 2010). Therefore, it can be concluded that the loss of intra-abdominal contrast was mainly due to emaciation, confirmed by a moderate to severe loss of lumbar musculature in most ferrets, peritonitis, mesenteric lymphadenopathy and/or by the presence of abdominal soft-tissue masses.

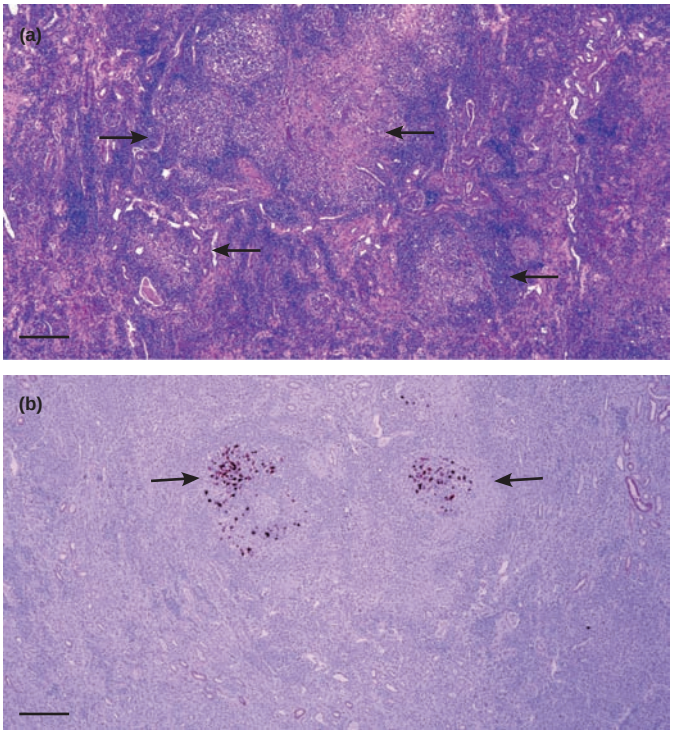

FIG 12: Image of the left kidney of the same ferret as in Fig 9. (a) Multifocal and coalescing granulomatous inflammation (arrows) are observed invading and compressing the adjacent parenchyma (haematoxylin and eosin staining). (b) Kidney: in the centre of the granulomas, numerous macrophages are observed with cytoplasmic immunoreactivity for coronavirus antigen (arrows). Immunohistochemistry (pictures courtesy of Dr. J. Martínez)

Peritonitis in ferrets may occur secondary to gastrointestinal perforation due to foreign body or proliferative bowel disease, secondary to carcinomatosis or secondary to ferret systemic coronavirus infection (Hoefer and others 1992, Darby and Ntavlourou 2006, Whittington and others 2006, Powers 2009, Murray and others 2010). In the present study, all lesions affecting the peritoneum, omentum and mesentery were clearly diagnosed as granulomatous peritonitis by means of histopathology.

A normal solitary mesenteric lymph node has been described in the mid-abdomen of ferrets. It is surrounded by a large amount of fat and located close to the cranial and caudal mesenteric veins. Normal mean dimensions (sd) of the large mesenteric lymph node are 12.6 mm (2.6) in length by 7.6 mm (2.0) in width. It is round to ovoid in shape and shows uniform echogenicity (Evans and An 1998, Paul-Murphy and others 1999). Although most of lymph nodes observed in this study were within normal limits (13.17 [1.74] mm in length by 8.32 [3.46] mm in width), they have been classified as abnormal because of their highly heterogeneous parenchyma or irregular shape and mixed echogenicity. Abdominal lymphadenopathy has also been reported in cats with FIP, but it seems to be less frequent than in ferrets. In the feline population studied by Lewis and O'Brien 2010, almost half of the cats did not have abdominal lymphadenopathy. Moreover, changes affecting the ultrasonographic appearance of the lymph nodes parenchyma have not been described in cats with FIP (Lewis and O'Brien 2010). Differentials for mesenteric lymphadenopathy in ferrets include: lymphosarcoma, inflammatory bowel disease and infectious diseases (Aleutian disease, multicentric cryptococcosis and FSCV) (Ohshima and others 1978, Welchman Dde and others 1993, Langlois 2005, Perpiñán and López 2008, Eshar and others 2010). In the present study, histopathological examination of the abnormal lymph nodes confirmed the diagnosis of granulomatous lymphadenitis, ruling out other possible aetiologies, such as fungal agents or mycobacteriosis. No correlation was found between the ultrasonographic appearance of the lymph nodes and the severity of the lesions.

In contrast with a previous FIP-study, where less than 20 per cent of cats show abdominal masses (Lewis and O'Brien 2010), ill-defined soft-tissue masses were recorded in 64 per cent of the ferrets positive for FSCV, on radiographs and/or ultrasound scans. In most cases, it was difficult to determine the origin of these masses because of their both radiographic and ultrasonographic heterogeneous appearance and the associated inflammatory changes reducing the imaging contrast. A contrast radiographic study may be useful in demonstrating the presence of abdominal masses when they produce external gastrointestinal obstruction or when they cause surrounding organ displacement, especially when ultrasound is not available (Schwarz and others 2003, Perpiñán and López 2008). Peritoneal granulomas or pyogranulomas (due to FSCV, fungal disease, foreign body), neoplasia (primary, such as lymphoma or metastatic) and lymphadenopathy should be included in the differential diagnosis of abdominal masses in ferrets (Cross 1987, Erdman and others 1992, 1996, Hoefer and others 1992, Lennox 2005, Darby and Ntavlourou 2006, Whittington and others 2006). Histopathology demonstrated that all of them were granulomas or pyogranulomas affecting the peritoneum, abdominal lymph nodes, small bowel, kidneys and pancreas.

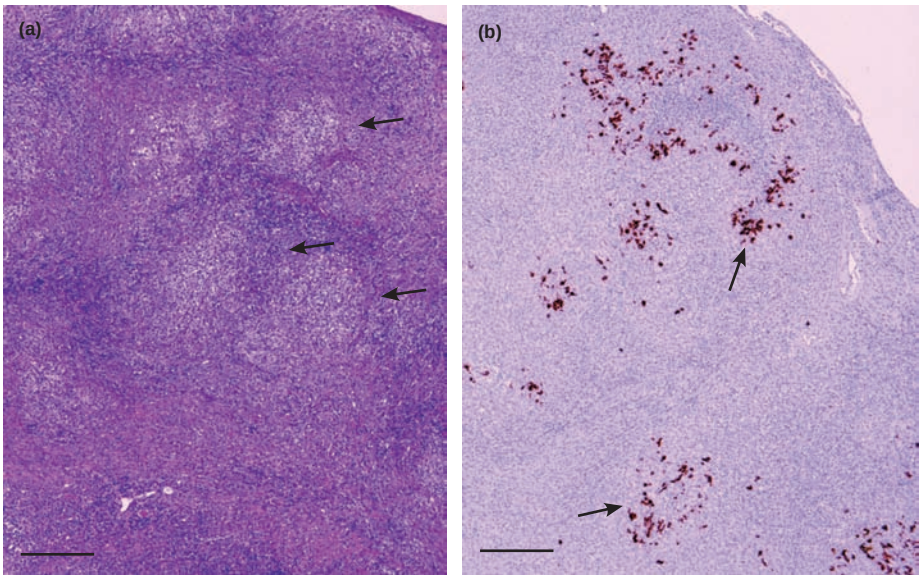

FIG 13: Lymph node. (a) The parenchyma is invaded and obliterated by a multifocal to coalescing granulomatous inflammatory reaction (black arrows). (haematoxylin and eosin staining). (b) These granulomas show numerous macrophages in the centre with cytoplasmic immunoreactivity for coronavirus antigen. Immunohistochemistry (pictures courtesy of Dr. J. Martínez)

Nephromegaly is a frequent finding in FIP and it has also been described in previous studies in ferrets (Perpiñán and López 2008, Lewis and O'Brien 2010, Murray and others 2010). Hydronephrosis and hydroureter are uncommon in ferrets and

most of the cases reported in the literature have been due to inadvertent ligation of the ureters during ovariohysterectomy. Other pathologies that can cause secondary hydronephrosis and hydroureter include ureteral and/or urethral obstruction caused by ureteral calculi, paraurethral cysts and/or prostatomegaly and hydronephrosis secondary to carcinoma of undetermined origin (Orcutt 2003, Pollock 2004). In the current study, four ferrets showed nephromegaly. From those, bilateral nephromegaly and hydroureter were observed in two cases (a neutered male and a neutered female) and signs of inflammatory perinephric infiltration were confirmed under ultrasound exam. In one of these patients (neutered male), the inflammatory reaction involved the bladder neck and extended towards the inguinal region, being accompanied by vascular thrombosis. Vasculitis, one of the most common inflammatory lesions in ferrets with FSCV, may be responsible for the changes observed in this ferret (Garner and others 2008, Martinez and others 2008, Addie and others 2009). The sonographic appearance of the bladder wall of this patient may be observed in other infiltrative processes, such as cystitis or neoplasia (Sutherland-Smith 2008). However, in this case, the most affected layer was the serosa, which corresponds with the visceral peritoneum. In the other case (neutered female), biopsy samples from the kidneys demonstrated the presence of granulomatous nephritis with positive IHC labelling. These results exclude the possibility of hydroureter secondary to inadvertent ligation during ovariohisterectomy.

As in the study describing FIP-affected cats, renal echogenicity was also variable in ferrets with FSCV, but none of them showed a hypoechoic subcapsular rim (Lewis and O'Brien 2010). Diffuse and/or cortical increase of the renal echogenicity has been associated with several renal diseases in dogs and cats (d'Anjou 2008). In ferrets, there are no studies evaluating these imaging findings and their correlation with histopathology. In the present study, five patients, with imaging renal changes had positive FRSCV granulomatous nephritis, a patient with nephromegaly and hyperechoic renal cortices had no histopathological renal lesions and other with severe nephromegaly did not have renal biopsy samples. On the other hand, one ferret, with confirmed granulomatous nephritis and positive IHC labelling in the renal tissue, did not show any renal abnormalities in the imaging examination. Unfortunately, urianalysis were not available in these cases.

In conclusion, in the current study, nephromegaly could be secondary to hydronephrosis and inflammatory infiltration of the kidneys. Hydronephrosis and hydroureter could be due to an obstructive effect caused by inflammatory infiltration around the ureters and the ureterovesical junction.

Cortical renal cysts were found in four patients. Solitary renal cysts are frequently seen as incidental findings during ultrasound examination or postmortem examination in ferrets. They are usually single or present in small numbers but in some cases can involve a large area of renal parenchyma. However, even relatively large renal cysts may be clinically insignificant (Orcutt 2003).

The intestinal serosa is one of the most commonly affected tissues in cases of FSCV (Murray and others 2010). At the same time, non-specific clinical signs, such as hyporexia or anorexia, weight loss, diarrhoea and vomiting, are commonly encountered in FSCV. In the present study, only one of the three patients that showed abnormal dilation of the gastrointestinal tract with gas had granulomatous enteritis; in a second one, gastrointestinal lesions were not observed neither at the postmortem examination nor at the histopathological study. The last one had no gastrointestinal biopsies. None of the ferrets showed thickening of the gastrointestinal tract or loss of the normal layering (Lewis and O'Brien 2010). On the other hand, two patients with confirmed granulomatous enteritis had no imaging lesions. Common causes of gastrointestinal diseases in ferrets include foreign body ingestion, bacterial infection (*Helicobacter mustelae*, *Salmonella* species, *Escherichia coli*), viral infection (ECE, Aleutian disease and rotavirus infection), parasitic infection, inflammatory bowel disease, gastrointestinal neoplasia, stress and idiopathic megaoesophagus (Lennox 2005). Abnormal gas patterns seen on radiographs can suggest obstruction by extraintestinal abdominal masses or mesenteric lymphadenopathy or may be secondary to enteritis (Williams and others 2000, Schwarz and others 2003).

As it occurs in cats with FIP, the liver is commonly affected in FSCV and may show hepatomegaly and multifocal nodules on the surface or inside the parenchyma (Lewis and O'Brien 2010, Murray and others 2010). In FIP imaging, the majority of livers were described as normal in both size and echogenicity. In the study described here, all ferrets had a normal liver size based on radiographic evaluation and normal parenchymal echogenicity. However, two patients that exhibited pyogranulomatous hepatitis on histopathological examination did not show imaging changes.

Splenomegaly and splenic nodules are commonly observed lesions in cases of FSCV (Murray and others 2010). In the present study, where splenomegaly was observed radiographically and/or ultrasonographically, the histopathological findings included fibronecrotising splenitis, ectopic spleen, splenic congestion, necrosis and pyogranulomatous splenitis (in this case, lymphoid hyperplasia and extramedullary haematopoiesis were also present). Moreover, one patient with splenomegaly had histopathologically normal spleen. It has been described that splenomegaly is a common finding in ferrets but is seldom of clinical importance. The most common histological diagnosis of enlarged spleens is extramedullary haematopoiesis. However, when a ferret is presented with non-specific symptoms and splenomegaly, ultrasound examination and ultrasound-guided biopsy are recommended (Schoemaker 2002). Ultrasound-guided biopsies were not performed in the present study as the ultrasound scans were performed in unsedated patients and surgical biopsies were considered safer and more likely to provide a definitive diagnosis.

In conclusion, although definitive diagnosis of systemic coronavirus infection is based on histological and immunohistochemical results, imaging techniques provide additional information that aids in the antemortem diagnosis of FSCV. Imaging signs of peritonitis and the presence of mesenteric lymphadenopathy and soft-tissue abdominal masses are highly suspicious of systemic coronavirus infection. As in cats with FIP, liver and spleen ultrasonographic data were not conclusive for the diagnosis of FSCV in ferrets. Aleutian disease, lymphoma, chronic inflammatory bowel disease, abdominal neoplasia, abdominal abscess, abdominal granulomas and mycobacteriosis should be included in the differential diagnosis of ferrets with these findings. As it has been described in cats, ultrasound is superior to radiology when abdominal contrast is reduced, as it frequently occurs in these cases. However, it can not replace histopathology in the definitive diagnosis.

Acknowledgements

This work was presented as an oral communication at the European Veterinary Diagnostic Imaging Annual Scientific Conference (Germany, July 2010), funded by one EAVDI (European Association of Veterinary Diagnostic Imaging) Travel Award 2010. The authors acknowledge Dr. J. Martínez from 'Servei de Diagnòstic de Patologia Veterinària' (Facultat de Veterinària, Universitat Autònoma de Barcelona, Spain) for his expert assistance with histological diagnosis.

Conflict of interest

None of the authors of this paper has a financial or personal relationship with other people or organisations that could inappropriately influence or bias the content of the paper.

References

ADDIE, D., BELÁK, S., BOUCRAUT-BARALON, C., EGBERINK, H., FRYMUS, T., GRUFFYDD-JONES, T. & OTHERS (2009) Feline infectious peritonitis. ABCD guidelines on prevention and management. *Journal of Feline Medicine and Surgery* **11,** 594-604

CROSS, B. M. (1987) Hepatic vascular neoplasms in a colony of ferrets. *Veterinary Pathology* **24,** 94-96

D'ANJOU, M. A. (2008) Kidneys and ureters. In Atlas of Small Animal Ultrasonography. Eds D. Pennick, M. A. d'Anjou. Blackwell Publishing. pp 339-364

DARBY, C. & NTAVLOUROU, V. (2006) Hepatic hemangiosarcoma in two ferrets (*Mustela putorius furo*). *Veterinary Clinics of North America: Exotic Animal Practice* **9,** 689-694

DENNIS, R. (2010) Handbook of Small Animal Radiology and Ultrasound. Techniques and Differential Diagnoses. Churchill Livingstone Elsevier

ERDMAN, S. E., BROWN, S. A., KAWASAKI, T. A., MOORE, F. M., LI, X. & FOX, J. G. (1996) Clinical and pathologic findings in ferrets with lymphoma: 60 cases (1982 to 1994). *Journal of the American Veterinary Medical Association* **208,** 1285-1289

ERDMAN, S. E., MOORE, F. M., ROSE, R. & FOX, J. G. (1992) Malignant lymphoma in ferrets: clinical and pathological findings in 19 cases. *Journal of Comparative Pathology* **106,** 37-47

ESHAR, D., MAYER, J., PARRY, N. M., WILLIAMS-FRITZE, M. J. & BRADWAY, D. S. (2010) Disseminated, histologically confirmed *Cryptococcus* species infection in a domestic ferret. *Journal of the American Veterinary Medical Association* **236,** 770-774

EVANS, H. E. & AN, N. Q. (1998) Anatomy of the ferret. In Biology and Diseases of the Ferret. Eds G. F. Fox. Lippincott Williams and Wikins. pp 19-69

FARROW, C. S. (2009) Veterinary Diagnostic Imaging: Birds, Exotic Pets and Wildlife. Mosby Elsevier

GARNER, M. M., RAMSELL, K., MORERA, N., JUAN-SALLÉS, C., JIMÉNEZ, J., ARDIACA, M. & OTHERS (2008) Clinicopathologic features of a systemic coronavirus-associated disease resembling feline infectious peritonitis in the domestic ferret (*Mustela putorius*). *Veterinary Pathology* **45,** 236-246

HOEFER, H. L., PATNAIK, A. K. & LEWIS, A. D. (1992) Pancreatic adenocarcinoma with metastasis in two ferrets. *Journal of the American Veterinary Medical Association* **201,** 466-467

LANGLOIS, I. (2005) Viral diseases of ferrets. *Veterinary Clinics of North America: Exotic Animal Practice* **8,** 139-160

LENNOX, A. M. (2005) Gastrointestinal diseases of the ferret. *Veterinary Clinics of North America: Exotic Animal Practice* **8,** 213-225

LEWIS, K. M. & O'BRIEN, R. T. (2010) Abdominal ultrasonographic findings associated with feline infectious peritonitis: a retrospective review of 16 cases. *Journal of the American Animal Hospital Association* **46,** 152-160

MARTÍNEZ, J., RAMIS, A. J., REINACHER, M. & PERPIÑÁN, D. (2006) Detection of feline infectious peritonitis virus-like antigen in ferrets. *Veterinary Record* **158,** 523

MARTÍNEZ, J., REINACHER, M., PERPIÑÁN, D. & RAMIS, A. (2008) Identification of group 1 coronavirus antigen in multisystemic granulomatous lesions in ferrets (*Mustela putorius furo*). *Journal of Comparative Pathology* **138,** 54-58

MURRAY, J., KIUPEL, M. & MAES, R. K. (2010) Ferret coronavirus-associated diseases. *Veterinary Clinics of North America: Exotic Animal Practice* **13,** 543-560

OHSHIMA, K., SHEN, D. T., HENSON, J. B. & GORHAM, J. R. (1978) Comparison of the lesions of Aleutian disease in mink and hypergammaglobulinemia in ferrets. *American Journal of Veterinary Research* **39,** 653-657

ORCUTT, C. J. (2003) Ferret urogenital diseases. *Veterinary Clinics of North America: Exotic Animal Practice* **6,** 113-138

PAUL-MURPHY, J., O'BRIEN, R. T., SPAETH, A., SULLIVAN, L. & DUBIELZIG, R. R. (1999) Ultrasonography and fine needle aspirate cytology of the mesenteric lymph node in normal domestic ferrets (*Mustela putorius furo*). *Veterinary Radiology & Ultrasound* **40,** 308-310

PERPIÑÁN, D. & LÓPEZ, C. (2008) Clinical aspects of systemic granulomatous inflammatory syndrome in ferrets (*Mustela putorius furo*). *Veterinary Record* **162,** 180-184

POLLOCK, C. G. (2004) Urogenital diseases in ferrets. In Ferrets, Rabbits and Rodents: Clinical Medicine and Surgery. Eds K. E. Quesenberry, J. W. Carpenter. Saunders Elsevier. pp 41-49

POWERS, L. V. (2009) Bacterial and parasitic diseases of ferrets. *Veterinary Clinics of North America: Exotic Animal Practice* **12,** 531-61

SCHOEMAKER N. J. (2002) Ferrets. In BSAVA Manual of Exotic Pets. 4th edn. Eds A. Meredith, S. Redrobe. BSAVA. pp 93

SCHWARZ, L. A., SOLANO, M., MANNING, A., MARINI, R. P. & FOX, J. G. (2003) The normal upper gastrointestinal examination in the ferret. *Veterinary Radiology & Ultrasound* **44,** 165-172

SUTHERLAND-SMITH, J. (2008) Bladder and urethra. In Atlas of Small Animal Ultrasonography. Eds D. Pennick, M. A. d'Anjou. Blackwell Publishing. pp 365-383

THRALL, D. E. (2007) Textbook of Veterinary Diagnostic Radiology. Saunders Elsevier

WELCHMAN, D. d. e. B., OXENHAM, M. & DONE, S. H. (1993) Aleutian disease in domestic ferrets: diagnostic findings and survey results. *Veterinary Record* **132,** 479-484

WHITTINGTON, J. K., EMERSON, J. A., SATKUS, T. M., TYAGI, G., BARGER, A. & PINKERTON, M. E. (2006) Exocrine pancreatic carcinoma and carcinomatosis with abdominal effusion containing mast cells in a ferret (*Mustela putorius furo*). *Veterinary Clinics of North America: Exotic Animal Practice* **9,** 643-650

WILLIAMS, B. H., KIUPEL, M., WEST, K. H., RAYMOND, J. T., GRANT, C. K. & GLICKMAN, L. T. (2000) Coronavirus-associated epizootic catarrhal enteritis in ferrets. *Journal of the American Veterinary Medical Association* **217,** 526-530

WISE, A. G., KIUPEL, M., GARNER, M. M., CLARK, A. K. & MAES, R. K. (2010) Comparative sequence analysis of the distal one-third of the genomes of a systemic and an enteric ferret coronavirus. *Virus Research* **149,** 42-50

WISE, A. G., KIUPEL, M. & MAES, R. K. (2006) Molecular characterization of a novel coronavirus associated with epizootic catarrhal enteritis (ECE) in ferrets. *Virology* **349,** 164-174

Veterinary Record

Abdominal radiographic and ultrasonographic findings in ferrets (*Mustela putorius furo*) with systemic coronavirus infection

E. Dominguez, R. Novellas, A. Moya, Y. Espada and J. Martorell

Veterinary Record 2011 169: 231 originally published online August 22, 2011
doi: 10.1136/vr.d4705

Notes